2015 International Symposium on Nonlinear Theory and its Applications
NOLTA2015, Kowloon, Hong Kong, China, December 1-4, 2015

Modulation frequency response in synchronized semiconductor lasers subject to constant-amplitude and random phase light

Kazutaka Kanno[†,1], Tohru Ariarakawa[†], Atsushi Uchida[‡,2], and Masatoshi Bunsen[†,3]

†Department of Electronics Engineering and Computer Science, Fukuoka University,
8-19-1 Nanakuma, Johnan-ku, Fukuoka, Japan
‡Department of Information and Computer Sciences, Saitama University,
255 Shimo-Okubo, Sakura-ku, Saitama City, Saitama, 338-8570, Japan
Email: [1]kkanno@fukuoka-u.ac.jp, [2]auchida@mail.saitama-u.ac.jp, [3]bunsen@fukuoka-u.ac.jp

Abstract—Dynamics and synchronization in semiconductor lasers subject to constant-amplitude and random phase light are numerically and analytically investigated. We particularly focus on frequency response of optical intensity to phase modulation for injected light. Lang-Kobayashi equations are used for our numerical simulation. Frequency spectra of time-series for optical intensity can be obtained from the numerical simulation, and our results are consistent with experimental ones shown in [1]. We also explain the frequency response by using linear stability analysis.

1. Introduction

It has been known that a common random input could give rise to synchronization between two uncoupled nonlinear dynamical systems [2]. This phenomenon is known as common random-signal induced synchronization. Semiconductor lasers are one of nonlinear dynamical systems which show such synchronization phenomenon [3].

Recently, a secure key distribution scheme using synchronization of semiconductor lasers has been proposed [4]. This scheme is implemented by using common signal induced synchronization in semiconductor lasers with constant-amplitude and random-phase (CARP) light [3]. A model of common signal induced synchronization using CARP light is shown in Fig. 1. The model consists of three semiconductor lasers. One laser is called drive, and other two lasers are called response 1 and response 2. The optical output of the drive laser has a constant amplitude. CARP light is generated by modulating electric phase of the optical output from the drive laser by using a noise signal. The CARP light is injected into the two response lasers. Optical intensity produced by the response lasers intricately fluctuates, but their temporal waveforms can be synchronized.

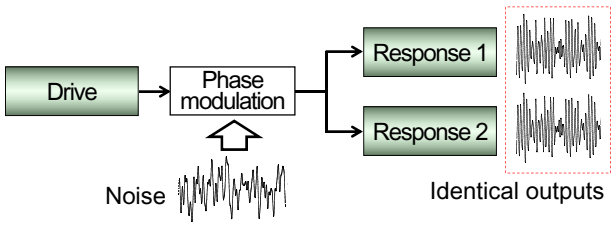

Figure 1: Model for common random signal induced synchronization in semiconductor lasers with CARP light.

For secure key distribution, it is required that measuring the optical phase of the CARP light is difficult. Enhancing the frequency bandwidth of the phase-modulation signal for the CARP light can be one of methods for making it difficult to measure the optical phase. Recently, dependence of both the synchronization and the dynamics of the response lasers on the frequency bandwidth of the phase-modulation signal has been experimentally investigated [1]. However, the mechanism of the dependence has not been cleared. In this study, we numerically confirm the dependence of both the synchronization and the dynamics of the response laser on the frequency bandwidth of the phase-modulation signal for CARP light. We also explain the mechanism of the dependence by linearizing a numerical model for the response laser.

2. Numerical model

The temporal dynamics of the two response lasers shown in Fig. 1 is governed by the Lang-Kobayashi equations as shown in the following [5]:

$$\frac{dE_{1,2}(t)}{dt} = \frac{1+i\alpha}{2}\left[G_N(N_{1,2}(t)-N_0)-\frac{1}{\tau_p}\right]E_{1,2}(t) + \kappa_{inj}E_{inj}(t)\exp[i(\Delta\omega t-\omega_d\tau_{inj})]+\xi_{1,2}(t), \quad (1)$$

$$\frac{dN_{1,2}(t)}{dt} = J_r-\frac{N_{1,2}(t)}{\tau_s}-G_N(N_{1,2}(t)-N_0)|E_{1,2}(t)|^2, \quad (2)$$

where E is the slowly varying complex electric amplitude and N is the carrier density. The subscripts 1 and 2 represents the response 1 and 2, respectively. Common parameters for the two response lasers have the subscript r. G_N is the gain coefficient, N_0 is the carrier density at transparency, α is the linewidth enhancement factor, τ_p is the photon lifetime, τ_s is the carrier lifetime, and J is the injection current. The injection current is given as $J = 1.5J_{th}$,

where J_{th} is that at the lasing threshold. Other parameter values are set to the same as in [6]

Optical injection to the response lasers is represented by the second term in the right hand side of Eq. (1). κ_{inj} is the injection strength and $\Delta\omega$ is the optical angular frequency detuning between the drive and the response. $\Delta\omega$ is given as $\Delta\omega = \omega_d - \omega_r$, where ω is the optical angular frequency. $\omega_d\tau_{inj}$ represents the phase shift due to the propagation of light from the drive. τ_{inj} is the propagation time, but $\tau_{inj} = 0$ is used for simplicity. Unless otherwise noted, $\kappa_{inj} = 31.1$ ns^{-1} and $\Delta f = -4.0$ GHz are used. Injection locking is achieved by using these parameter values.

$E_{inj}(t)$ for optical injection represents the CARP light and is given by the following equations,

$$E_{inj}(t) = A_d \exp[i\eta_{lpf}(t)], \tag{3}$$

where A_d is the electric amplitude of the drive laser and is temporally constant. $\eta_{lpf}(t)$ represents the phase-modulation signal for the CARP light. $\eta_{lpf}(t)$ is generated by passing a colored noise $\eta(t)$ through a lowpass filter with a cutoff frequency f_c. The colored noise $\eta(t)$ is generated by the Ornstein-Uhlenbeck process shown in the following differential equation,

$$\frac{d\eta(t)}{dt} = -\frac{\eta(t)}{\tau_m} + \sqrt{\frac{2}{\tau_m}}\xi_m(t), \tag{4}$$

where $\tau_m = 0.02$ ns is a positive constant. $\xi_m(t)$ is the normalized white Gaussian noise with the properties $\langle\xi_m(t)\rangle = 0$ and $\langle\xi_m(t)\xi_m(s)\rangle = \delta(t-s)$, where $\langle\cdot\rangle$ denotes the ensemble average and δ is the Dirac's delta function. $\eta(t)$ has the properties $\langle\eta(t)\rangle = 0$ and $\langle\eta(t)\eta(s)\rangle = \exp[-|t-s|/\tau_m]$. The characteristic time of $\eta(t)$ is defined by τ_m.

In this study, the lowpass filter is realized by using a digital filter. We use a finite impulse response filter with hanning window as the digital filter.

The third term $\xi_{1,2}(t)$ in the right hand side of Eq. (1) represents spontaneous emission. $\xi_{1,2}(t)$ is complex number, and degenerates synchronization accuracy in our model.

3. Derivation of amplitude response to CARP light in semiconductor lasers

We derive the frequency response of the electric amplitude to the phase modulation for the CARP light by linearizing the Lang-Kobayashi equations. The two response lasers are synchronized by a common input signal. Since the synchronization is achieved by injection locking, we consider steady state solutions for an injection locked laser.

Firstly, we assume that the optical phase of the common input signal is not modulated, which gives $E_{inj}(t) = A_d$ in Eq. (1). We consider the steady state solutions for $E(t)$ and $N(t)$ as $E(t) = A_s \exp[i(\Delta\omega t + \phi_s)]$, where $\Delta\omega t$ comes from injection locking, and $N(t) = N_s$. Inserting the solutions and $E_{inj}(t) = A_d$ into Eqs. (1) and (2) gives us the following solutions,

$$|A_s|^2 = \frac{jN_{th} - N_s}{\tau_s G_N (N_s - N_0)}, \tag{5}$$

$$\phi_s = \sin^{-1}\left[\frac{-\Delta\omega}{\kappa_{inj}\sqrt{1+\alpha^2}}\right] - \tan^{-1}\alpha, \tag{6}$$

$$N_s = N_{th} - \frac{2\kappa_{inj}\cos\phi_s}{G_N}, \tag{7}$$

where we used $A_d = A_s$ for the injected field to simplify our analysis.

Next, we consider small perturbations written in the form $x(t) = x_s + \delta x(t)$ ($x = A$, ϕ, and N) in order to investigate the stability of the injected laser. We assume the signal term that also takes the form $E_{inj}(t) = A_d \exp[i(\delta\phi_{drv}(t))]$. Inserting these variables into Eqs. (1) and (2) leads to the following set of linearized equations:

$$\frac{d\delta A(t)}{dt} = a_1\delta A(t) + a_2\delta\phi(t) + a_3\delta N(t) + a_2\delta\phi_{drv}(t), \tag{8}$$

$$\frac{d\delta\phi(t)}{dt} = a_4\delta A(t) + a_1\delta\phi(t) + a_5\delta N(t) + a_1\delta\phi_{drv}(t), \tag{9}$$

$$\frac{d\delta N(t)}{dt} = a_6\delta A(t) + a_7\delta N(t), \tag{10}$$

where

$$\begin{aligned} &a_1 = -\kappa_{inj}\cos[\phi_s], \quad a_2 = -\kappa_{inj}A_s\sin[\phi_s], \quad a_3 = \frac{G_N A_s}{2}, \\ &a_4 = \frac{\kappa_{inj}}{A_s}\sin[\phi_s], \qquad\qquad a_5 = \frac{\alpha G_N}{2}, \\ &a_6 = -2G_N A_s(N_s - N_0), \quad a_7 = -\frac{1}{\tau_s} - G_N A_s^2. \end{aligned} \tag{11}$$

Since we are interested in the frequency response, we replace the small perturbation $\delta x(t)$ into $\delta x_c \exp[i\omega_{in}t]$, where x is A, ϕ, N, or ϕ_{drv}. In the transform, ω_{in} is the angular frequency of the perturbation. Inserting $\delta x(t) = \delta x_c \exp[i\omega_{th}]t$ into Eqs. (8)–(10), the frequency response of the electric amplitude to the phase modulation for the CARP light is represented as shown in the following equation:

$$\frac{\delta A_c}{\delta\phi_{drv,c}} = \frac{(i\omega_{in} - a_7)a_2 i\omega_{in}}{D(\omega_{in})}, \tag{12}$$

where

$$\begin{aligned} D(\omega_{in}) = &(i\omega_{in} - a_1)(i\omega_{in} - a_1)(i\omega_{in} - a_7) - a_2a_5a_6 \\ &- (i\omega_{in} - a_1)a_3a_6 - (i\omega_{in} - a_7)a_2a_4. \end{aligned} \tag{13}$$

Eq. (12) is complex number and we calculate its absolute value.

4. Numerical results

We show examples of signals used for modulating the optical phase of input signals injected into the response laser. Figure 2 shows temporal waveforms and frequency

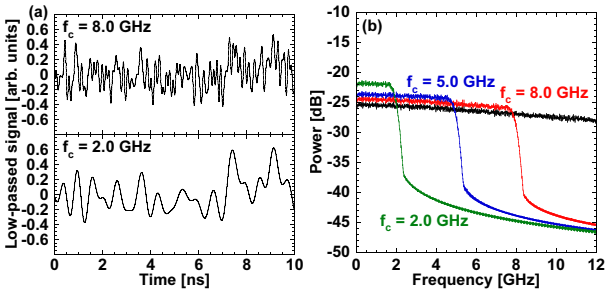

Figure 2: Examples of the phase-modulation signal passed through the lowpass filter with different cutoff frequency f_c. (a) is the temporal waveforms. (b) is the frequency spectra, but the black curve is not filtered. The cutoff frequencies f_c = 2.0, 5.0, and 8.0 GHz are used.

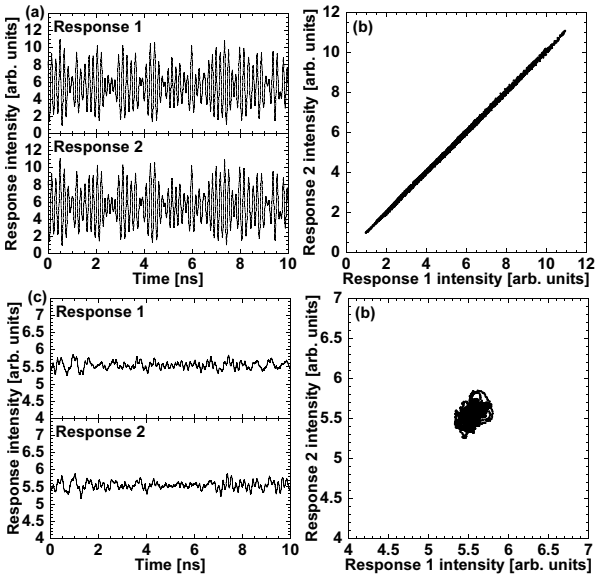

Figure 3: Temporal waveforms of the response lasers and their correlation plots. The cutoff frequency f_c for the CARP light is 8.0 GHz for (a) and (b). f_c = 2.0 GHz is used for (c) and (d)..

spectra of the signals for the modulation. In the upper and lower panel of Fig. 2(a), the lowpass filter with f_c = 8.0 and 2.0 GHz is used, respectively. The amplitude of the phase-modulation signal is normalized so that the standard deviation of the amplitude is 0.2. Fig. 2(b) shows the frequency spectra corresponding to the temporal waveforms. We can see that power is reduced in larger frequency than f_c.

By injecting CARP light into the two response lasers, synchronization between them is achieved. Figure 3 shows temporal waveforms of the response 1 and 2 and their correlation plot. For Figs. 3(a) and 3(b), the cutoff frequency f_c = 8.0 GHz is used for generating the phase-modulation signal. The two temporal waveforms are strongly correlated as shown in Fig. 3(a) and (b), and synchronization is achieved. On the other hand, Figs. 3(c) and 3(d) are for

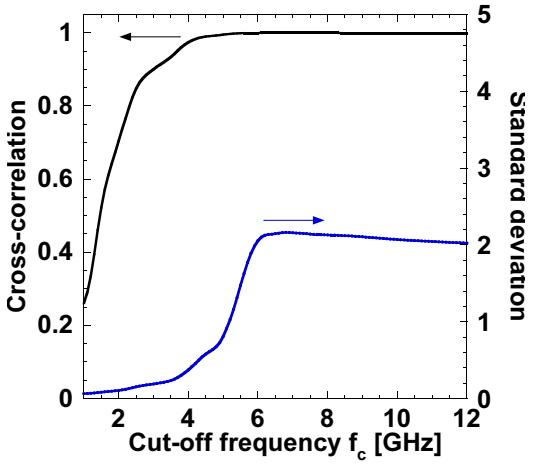

Figure 4: Dependence of the cross-correlation value C and the standard deviation of the temporal output of the response 1 laser on the cutoff frequency f_c.

f_c = 2.0 GHz. We find that the temporal waveforms are weakly correlated and the their amplitude is smaller than those of Fig. 3(a).

We introduce a cross-correlation value to evaluate synchronization accuracy.

$$C = \frac{\left\langle (I_1(t) - \bar{I}_1)(I_2(t) - \bar{I}_2) \right\rangle}{\sigma_1 \sigma_2} \tag{14}$$

In this equation, $I(t)$ is the optical intensity, $\bar{I}$ is the mean value of $I(t)$, σ is the standard deviation of $I(t)$, and $\langle \cdot \rangle$ indicates time averaging.

The black curve in Figure 4 depicts the dependence of the cross correlation value C on f_c. High values of C (almost one) is obtained for $f_c > 6$ GHz. However, C is relatively low for small f_c. The reason for low values of C is the small amplitudes of the temporal waveforms of the response lasers. The blue curve in Fig. 4 represents the standard deviation of the temporal waveform of the response 1 laser versus f_c. The standard deviation is small for small f_c. When the standard deviation is small, noise effect due to spontaneous emission becomes relatively large. The noise effect degenerates synchronization accuracy.

Next, we investigate the frequency response of the semiconductor laser with the CARP light. Figure 5(a) shows the frequency response calculated by using Eq. (12). We find that the spectrum has a resonance peak at 5.8 GHz. This peak corresponds to a damping oscillation mode for injection locked semiconductor lasers [7]. We compare the analytical result with numerically obtained frequency spectra. Fig. 5(b) shows the frequency spectrum of the response laser when the phase-modulation signal is not filtered. The spectrum has a resonance peak at 5.6 GHz, which corresponds to the peak at 5.8 GHz for Fig. 5(a), and the shape of the spectrum is similar to Fig. 5(a).

Figures 5(c) and 5(d) show the frequency spectra at f_c = 8.0 GHz and 2.0 GHz. We find that the power drop

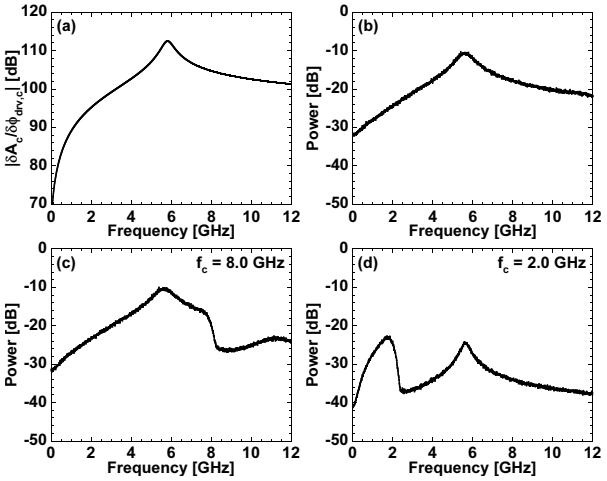

Figure 5: (a) is the frequency response calculated from Eq. (12). (b)–(d) are numerically obtained frequency spectra of the response 1 laser. The phase-modulation signal is not filtered for (b). The frequency bandwidth of the phase-modulation signal for (c) and (d) are limited by using the lowpass filter with f_c = 8.0 GHz and 2.0 GHz, respectively.

at the frequency corresponding to f_c. The response laser has the frequency response under f_c in Fig. 5(a) since the phase-modulation signal has oscillation with the lower frequencies than f_c. The frequency spectra for lower frequencies than f_c have similar shape to Fig. 5(a). This means that the response laser has frequency spectra that are obtained by passing a noise signal with flat frequency spectrum through the transform of Fig. 5(a). However, the peak at 5.6 GHz is still observed even for f_c = 2.0 GHz. This peak comes from relaxation oscillation frequency for injection locked semiconductor lasers.

The reason for low values of the standard deviation for small f_c in Fig. 4 is because of low frequency response for small frequency in Fig. 5(a). When f_c is small, the frequency response for lower frequency than f_c is obtained as shown in Fig. 5(d). The magnitude of the power at the lower frequencies of Fig. 5(d) is comparable to the peak at 5.6 GHz. The peak comes from the relaxation oscillation produced by spontaneous emission noise. Since the power for both the noise and the lower frequencies has similar magnitude, the noise is relatively large. Therefore, the cross correlation value decays.

Finally, we investigate the dependence of the frequency response on the injection strength κ_{inj}. Figures 6(a) and (b) show the analytical and numerical result for the frequency response when the phase-modulation signal is not filtered, respectively. κ_{inj} = 31.1 ns^{-1}, 46.6 ns^{-1}, and 62.1 ns^{-1} are used in Fig. 6. The resonance peak becomes suppressed and the spectrum structure becomes almost flat when the injection strength is increased. We consider that the resonance suppression is due to enhanced damping of the linear mode [7]. The similar tendency is observed for the numerical result shown in Fig. 6(b).

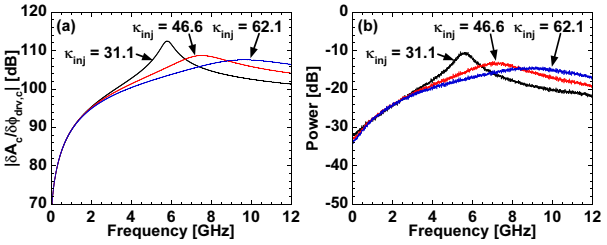

Figure 6: (a) is the frequency response calculated from Eq. (12). (b) is the numerically obtained frequency spectra of the temporal output of the response 1 laser. The injection strength κ_{inj} = 31.1 ns^{-1}, 46.6 ns^{-1}, and 62.1 ns^{-1} are used in these figures.

5. Conclusion

We numerically investigate the dependence of the synchronization of the response lasers on the frequency bandwidth of the phase-modulation signal for CARP light. We found that high correlation values are observed when the phase-modulation signal has large frequency bandwidths. However, narrow bandwidth of the phase-modulation signal degenerates the cross correlation value.

We also show the dependence of the frequency spectra of the response laser on the frequency bandwidth and analytically investigate the dependence by a linear stability analysis. The stability analysis gives us the frequency response of the electric amplitude of the response laser to the phase modulation for the CARP light. The frequency response has a resonance peak which becomes suppressed when the injection strength is increased. The calculated frequency spectra of the response laser correspond to the analytical frequency response.

References

[1] I. Kakesu, N. Suzuki, A. Uchida, K. Yoshimura, K. Arai, and P. Davis, Proceedings of 2014 the International Symposium on Nonlinear Theory and Its Applications, vol.1, pp. 466–469 (2014).

[2] C. Zhou and J. Kurths, Phys. Rev. Lett., vol. 88, pp. 230602 (2002).

[3] H. Aida, M. Arahata, H. Okumura, H. Koizumi, A. Uchida, K. Yoshimura, J. Muramatsu, , and P. Davis, Optics Express, vol. 20, pp. 11813–11829 (2012).

[4] K. Yoshimura, J. Muramatsu, P. Davis, T. Harayama, H. Okumura, S. Morikatsu, H. Aida, and A. Uchida, Phys. Rev. Lett., vol. 108, pp. 070602 (2012).

[5] R. Lang and K. Kobayashi, IEEE Journal of Quantum Electronics, vol. 16, pp. 347–355 (1980).

[6] K. Kanno and A. Uchida, Phys. Rev. E, vol. 86, pp. 066202 (2012).

[7] A. Murakami, Phys. Rev. E, vol. 65, pp. 056617 (2002).